

1 **A homogenized daily *in situ* PM_{2.5} concentration dataset from national air quality**
2 **monitoring network in China**

3

4 Kaixu Bai^{1,2,3}, Ke Li³, Chengbo Wu³, Ni-Bin Chang⁴, Jianping Guo^{5*}

5

6 ¹Key Laboratory of Geographic Information Science (Ministry of Education), East China Normal University,
7 Shanghai, China

8 ²Institute of Eco-Chongming, 20 Cuiniao Rd., Chongming, Shanghai, China

9 ³School of Geographic Sciences, East China Normal University, Shanghai, China

10 ⁴Department of Civil, Environmental, and Construction Engineering, University of Central Florida, Orlando,
11 FL, USA

12 ⁵State Key Laboratory of Severe Weather, Chinese Academy of Meteorological Sciences, Beijing, China

13

14

15

16 *Correspondence to: Dr./Prof. Jianping Guo (jpguocams@gmail.com)

17

18

19
20
21
22
23
24
25
26
27
28
29
30
31
32
33
34
35
36
37
38
39

Abstract

In situ PM_{2.5} concentration observations have long been used as critical data sources in haze related studies. Due to the frequently occurred haze pollution events, China started to regularly monitor PM_{2.5} concentration nationwide from the newly established air quality monitoring network since 2013. Nevertheless, the acquisition of these invaluable air quality samples is challenging given the absence of public available data download interface. In this study, we provided a homogenized *in situ* PM_{2.5} concentration dataset that was created on the basis of hourly PM_{2.5} data retrieved from the China National Environmental Monitoring Center (CNEMC) via a web crawler between 2015 and 2019. Methods involving missing value imputation, change point detection, and bias adjustment were applied sequentially to deal with data gaps and inhomogeneities in raw PM_{2.5} observations. After excluding records with limited samples, a homogenized PM_{2.5} concentration dataset comprising of 1,309 five-year long PM_{2.5} data series at a daily resolution was eventually compiled. This is the first thrust to homogenize *in situ* PM_{2.5} observations in China. The trend estimations derived from the homogenized dataset indicate a spatially homogeneous decreasing tendency of PM_{2.5} across China at a mean rate of about -7.6% per year from 2015 to 2019. In contrast to raw PM_{2.5} observations, the homogenized data record not only has a complete data integrity but is more consistent over space and time. This homogenized daily *in situ* PM_{2.5} concentration dataset is publicly accessible at <https://doi.pangaea.de/10.1594/PANGAEA.917557> (Bai et al., 2020a), which can be applied as a promising dataset for PM_{2.5} related studies such as satellite-based PM_{2.5} mapping, human exposure risk assessment, and air quality management.

Keywords: PM_{2.5}; Data homogenization; Bias correction; *In situ* observation; Air quality indicators

40 **1 Introduction**

41 A consistent PM_{2.5} concentration dataset is vital to the analysis of variations in PM_{2.5} loadings
42 over space and time as well as in support of its risk analysis for air quality management, meteorological
43 forecasting, and health-related exposure assessment (Lelieveld et al., 2015; Yin et al., 2020). Ground-
44 based monitoring network is commonly built to measure concentrations of air pollutants across the
45 globe. Suffering from extensive and severe haze pollution events in the past few years (Guo et al.,
46 2014; Ding et al., 2016; Wang et al., 2016; Cai et al., 2017; Huang et al., 2018; Luan et al., 2018; Ning
47 et al., 2018), China launched the operational ambient air quality sampling late in 2012 on the basis of
48 the sparsely distributed aerosol observation network. To date, this *in situ* network has been enlarged
49 to cover almost all major cities in China consisting of about 1500 monitoring stations. Concentrations
50 of six key air pollutants including PM_{2.5}, PM₁₀, NO₂, SO₂, CO, and O₃, are routinely measured on an
51 hourly basis while the sampled data are released publicly online by the China National Environmental
52 Monitoring Center (CNEMC) since 2013.

53 Although *in situ* PM_{2.5} concentration data have played critical roles in improving our
54 understanding of regional air quality variations and relevant influential factors (Yang D. et al., 2018;
55 Yang Q. et al., 2019; Zheng et al., 2017), little concern was raised to the quality of such dataset itself
56 (Bai et al., 2019a, 2019c; He and Huang, 2018; Zhang et al., 2019, 2018; Zou et al., 2016). Meanwhile,
57 few studies provided a detailed description of the accuracy or bias level (uncertainty) of the observed
58 PM_{2.5} data in recent years (Xin et al., 2015; You et al., 2016; Guo et al., 2017; Shen et al., 2018). The
59 primary reason lies in the fact that neither quality assurance flag nor metadata information
60 documenting the uncertainty other than data samplings were provided, making such quality assessment
61 infeasible.

62 The data quality, in particular the data homogeneity, is of critical importance to the exploration
63 of the given dataset, especially for trend analysis (Bai et al., 2019c; C. Lin et al., 2018; Liu et al., 2018;
64 Ma et al., 2015) and data integration (Bai et al., 2019b, 2020b; T. Li et al., 2017; Zhang et al., 2019)
65 in which a homogeneous dataset is absolutely essential for downstream applications. Since two distinct
66 kinds of instruments are used in the current air quality monitoring network to measure near surface

67 PM_{2.5} concentration in China (Bai et al., 2020), imperfect instrumental calibration and intermittent
68 replacement of instruments may thus introduce obvious issue of discontinuity in PM_{2.5} observations.
69 Such inhomogeneity may result in large uncertainty and even biased results in the subsequent analysis,
70 especially in context-based and data driven PM_{2.5} concentration mapping (Bai et al., 2019b, 2019a; He
71 and Huang, 2018; Wei et al., 2020), in which *in situ* PM_{2.5} concentration observations are used as the
72 ground truth to characterize complex statistical relationships with other possible contributing factors.

73 Given the absence of an open access and quality assured *in situ* PM_{2.5} concentration dataset in
74 China, in this study, we attempted to generate a long-term coherent *in situ* PM_{2.5} concentration dataset
75 for scientific community to use in future applications. A set of methods involving missing value
76 imputation, change point detection, and bias adjustment were geared up seamlessly in a big data
77 analytic manner toward the improvement of data integrity and the removal of possible discontinuities
78 in raw PM_{2.5} observations. Such an analytical process is also referred to as data homogenization in
79 data science or big data analytics (Cao and Yan, 2012; Wang et al., 2007). To our knowledge, this is
80 the first thrust to homogenize a large-scale dataset of *in situ* PM_{2.5} concentration observations in China.
81 In the following sections, we will introduce the data source as well as detailed big data analytics
82 methods used for the creation of a homogenized PM_{2.5} concentration dataset.

83 **2 *In situ* PM_{2.5} concentration observations**

84 In this study, the hourly PM_{2.5} concentration data sampled from more than 1,600 state-controlled
85 air quality monitoring stations across China between January 1, 2015 and December 31, 2019 were
86 utilized. These PM_{2.5} concentration data were measured on an hourly basis using either beta-
87 attenuation monitors or Tapered Element Oscillating Microbalance (TEOM) analyzer. The ordinary
88 instrumental calibration and quality control were performed according to the national ambient air
89 quality standard of GB3095-2012 and HJ 618–2011 (Guo et al., 2009, 2017). Generally, TEOM can
90 measure PM_{2.5} concentration within the range of 0–5,000 $\mu\text{g m}^{-3}$ at a resolution of 0.1 $\mu\text{g m}^{-3}$, with
91 precisions of $\pm 0.5 \mu\text{g m}^{-3}$ for 24-h average and $\pm 1.5 \mu\text{g m}^{-3}$ for hourly average (Guo et al., 2017; Xin
92 et al., 2012; Xin et al., 2015). The PM_{2.5} measurements were publicly released online by the China

93 National Environmental Monitoring Center (CNEMC) via the National Urban Air Quality Real-time
94 Publishing Platform (<http://106.37.208.233:20035/>) within one hour after the direct sampling.

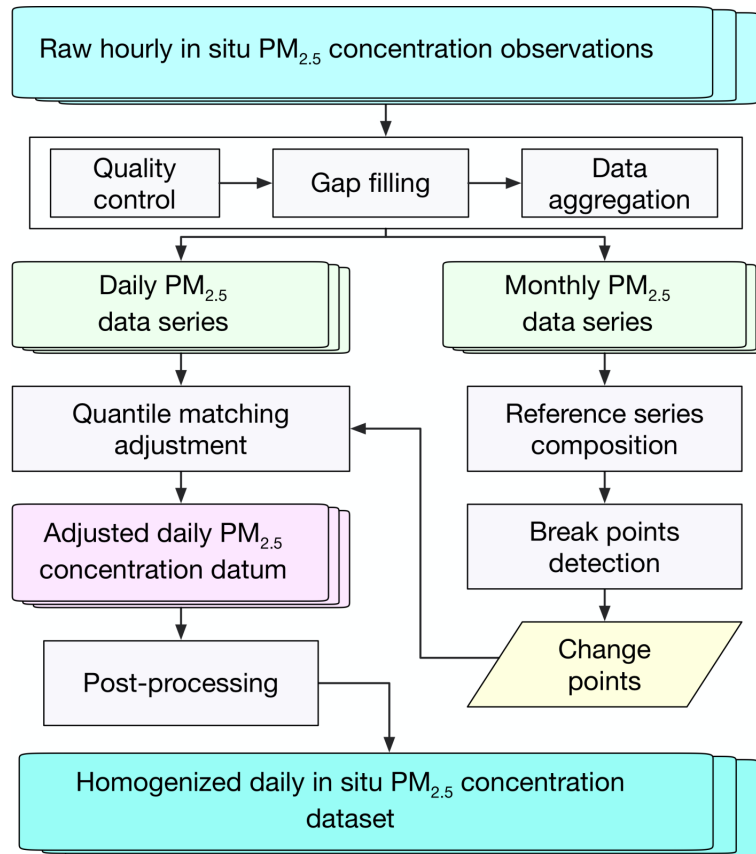
95 Although the sampled data were publicly released, the acquisition of these valuable samplings is
96 always challenging because no data download interface is provided to the public by the CNEMC
97 website. Therefore, it is impossible for users to retrieve the historical observations from the given
98 website. Rather, science community has to count on other measures such as an automatic web crawler
99 for the retrieval of these online updated data samples from the data publishing platform. Nevertheless,
100 the data records retrieved through such an approach suffered from significant data losses due to various
101 unexpected reasons like power outage and internet interruption. Consequently, the data integrity
102 becomes problematic and further treatments like gap filling are thus essential to accounting for such
103 defects at least.

104 Moreover, hourly PM_{2.5} concentration observations that were sampled at five embassies of United
105 States in China from January 2015 to June 2017 were used as an independent dataset to evaluate the
106 fidelity of the homogenized PM_{2.5} concentration dataset. Geographic locations of these five embassies
107 have been shown in Table S1. These PM_{2.5} data were measured independently under the U.S.
108 department of state air quality monitoring program and can be acquired from the
109 <http://www.stateair.net/>. To be in line with the homogenized dataset, the hourly PM_{2.5} concentration
110 data were aggregated to the daily level by averaging the 24-h observations sampled on each date while
111 daily averages were calculated only for days with more than 12 valid samples of a possible 24-h.

112 **3 Homogenization of *in situ* PM_{2.5} concentration data**

113 For the creation of a long-term coherent *in situ* PM_{2.5} concentration dataset, it is necessary to
114 create an analytical framework of the big data analytics which seamlessly gears up several methods as
115 a whole for the purposes of missing value imputation, change point detection, and discontinuity
116 adjustment, given the presence of data gaps and possible discontinuity in raw PM_{2.5} observations .
117 Figure 1 shows a schematic illustration of the general workflow toward generating a homogenized
118 PM_{2.5} concentration dataset and the whole process can be outlined as follows.

119 (1) It is necessary to perform essential quality control and gap filling on raw $PM_{2.5}$ observations so
 120 that the bias arising from large outliers and resampling errors due to incomplete observations can
 121 be reduced.



122
 123 **Figure 1.** A schematic flowchart for the creation of a homogenized daily *in situ* $PM_{2.5}$ concentration
 124 dataset.

125
 126 (2) Short-term time series due to sites relocation were temporally merged to attain a long-term record.
 127 Then, $PM_{2.5}$ concentration time series with a temporal coverage of less than four-year during the
 128 study period were excluded. Subsequently, the quality-controlled observations of hourly *in situ*
 129 $PM_{2.5}$ concentrations were resampled to daily and monthly scales to initiate the homogeneity test.

130 (3) Reference time series were constructed for each long-term $PM_{2.5}$ concentration record on the basis
 131 of data measured from adjacent monitoring sites. For $PM_{2.5}$ concentration records failing to
 132 produce a reliable reference series, no homogeneity test was performed for such datum due to the
 133 absence of essential reference data series.

134 (4) The discontinuity identified in each daily long-term PM_{2.5} concentration time series were corrected
135 using the quantile-matching (QM) adjustment method according to the change points detected in
136 each monthly data record with the support of reference series.

137 (5) Post-processing measures such as nonpositive value correction and another round gap filling were
138 further performed on the homogenized records to attain a quality-assured *in situ* PM_{2.5}
139 concentration dataset. More details of each analytic method were described in the following
140 subsections.

141 **3.1 Quality control**

142 Given the possibility of the presence of abnormal samplings, it is necessary to remove the outliers
143 detected in raw PM_{2.5} observations to reduce the false alarm rate in change point detection during the
144 subsequent homogeneity test. Specifically, hourly PM_{2.5} concentration data values meeting one of the
145 following criteria were excluded: 1) out of the range between 1 and 1,000 $\mu\text{g m}^{-3}$, and 2) more than
146 three standard deviations from the median of observations within a 15-h time window. Both criteria
147 aimed to remove large outliers which could result in biased daily averages. Overall, 3.46% of PM_{2.5}
148 samples were treated as outliers and were then excluded accordingly (treated as missing values).

149 **3.2 Gap filling and resampling**

150 As indicated in our recent study (Bai et al., 2020b), missing value related data gaps become a
151 big obstacle in the exploitation of raw PM_{2.5} observations that were retrieved from the CNEMC website
152 as PM_{2.5} observations on 40% of sampling days suffered from data losses due to unexpected reasons.
153 To reduce the impact of missing value related sampling (from hourly to daily) bias on the subsequent
154 homogeneity test, we filled those missing value related data gaps that were found in each 24-h PM_{2.5}
155 observations by applying the DCCEOF method developed very recently (Bai et al., 2020b). Such a
156 gap filling effort enabled us to improve the percentage of days without missingness during the study
157 time period from 58.8% to 97.3%.

158 In spite of the improvement of data integrity after gap filling, the resultant PM_{2.5} time series
159 remain temporally discontinuous due to the emergence of several long-lasting (e.g., more than 24
160 consecutive hours) data missing episodes. Also, the hourly time series are still too noisy to be handled

161 by the current homogeneity test software due to the significant variation in PM_{2.5} concentration over
162 space and time. In such context, the hourly PM_{2.5} concentration records were aggregated to daily and
163 monthly scales to initiate the homogeneity test. Moreover, the monthly series was primarily used to
164 detect the possible change points while the daily series was adjusted in reference to the corresponding
165 reference series based on the change points detected from the monthly series. To avoid large
166 resampling bias, monthly averages were calculated only for those with at least 20 valid daily means of
167 a possible month at each site. The frequency of missing values in each month was also calculated as a
168 possible metadata information to further examine the detected change points.

169 **3.3 Homogeneity test**

170 A commonly used homogeneity test software, the RHtestsV4 package, was hereby applied to
171 detect the possible discontinuities in raw PM_{2.5} data series that were retrieved from the CNEMC
172 website. As suggested in Wang and Feng (2013), RHtestsV4 is capable of detecting and adjusting
173 change points in a data series with first-order autoregressive errors. Given the low false alarm rate via
174 change point detection and the capability to adjust discontinuity, the RHtests software packages have
175 been widely used to homogenize climate data records such as temperature (Cao et al., 2013; Xu et al.,
176 2013; Zhao et al., 2014), precipitation (Wang et al., 2010a; Nie et al., 2019), and other datum like
177 boundary layer height (Wang and Wang, 2016). Two typical methods, namely the PMTred and
178 PMFred, were embedded in a recursive testing algorithm in RHtestsV4, with the former relying on the
179 penalized maximal t test (PMT) while the latter based on the penalized maximal F test (PMF) (Wang
180 et al., 2007; Wang, 2008a). With the incorporation of these empirical penalty functions (Wang, 2008a,
181 b), the problem of uneven distribution of false alarm rate is largely alleviated with the aid of RHtestsV4.
182 In contrast to the PMF which works without a reference series, the PMT uses a reference series to
183 detect change points and the results are thus far more reliable (Wang, 2008a, b). The way to generate
184 reference series will be described in the next subsection. Also, the RHtestsV4 is capable of making
185 essential adjustments to the detected discontinuities by taking advantage of the QM adjustment method
186 (Wang and Feng, 2013).

187 Here the PMT method rather than the PMF was used to detect change points given the higher
188 confidence of the former method in change point detection due to the involvement of reference series
189 (Wang and Feng, 2013). To ensure the reliability of detected discontinuities, change point was defined
190 and confirmed at a nominal 99% confidence level, and the data records were then declared to be
191 homogeneous once no change point was identified. Subsequently, the QM adjustment method was
192 applied to correct PM_{2.5} observations with evident drifts with the support of reference series, namely,
193 to homogenize PM_{2.5} concentration data series. To avoid large sampling uncertainty in the estimate of
194 QM adjustments, the Mq (i.e., the number of categories on which the empirical cumulative distribution
195 function is estimated) was automatically determined by the software to ensure adequate samples for
196 the estimation of mean difference and probability density function. Meanwhile, the number to
197 determine the base segment (i.e., $Iadj$) was set to zero so that datum in other segments were all adjusted
198 to the segment with the longest temporal coverage.

199 **3.3.1 Construction of reference series**

200 A good reference series is vital to the relative homogeneity test because it helps pinpoint possible
201 discontinuities in each base series (the data series to be tested) and determines the performance of the
202 subsequent data adjustment. In general, reference series can be organized by using one specific record
203 either measured from one adjacent station or aggregated from multiple observations (Cao and Yan,
204 2012; Peterson and Easterling, 1994; Xu et al., 2013; Wang et al., 2016). The most straightforward
205 way is to use the neighboring data series either measured at the nearest station or series that are highly
206 correlated with the base series (Peterson and Easterling, 1994; Cao and Yan, 2012; Wang and Feng,
207 2013). Such methods, however, fail to take the representativeness of the neighboring series into
208 account since the neighboring series may also suffer from discontinuities.

209 To avoid the misuse of inhomogeneous PM_{2.5} concentration records as reference series, a
210 complex yet robust data integration scheme was hereby developed to screen, organize, and construct
211 reference series for each *in situ* PM_{2.5} concentration data series. For each daily PM_{2.5} concentration
212 data series, all the neighboring series were firstly identified from its surroundings with a lag distance
213 as large as of 50 km. No reference series was constructed once there was no neighboring series
214 available within the given radius and in turn the homogeneity of the given record was not examined.

215 Otherwise, both correlation coefficient (R) and coefficient of variation (CV) were calculated between
216 the given base series and each selected neighboring series to assess their representativeness (Shi et al.,
217 2018; Rodriguez et al., 2019). Then, neighboring series with R greater than 0.8 and CV smaller than
218 0.2 were selected as candidates to construct the reference series for a given base series.

219 The reference series was then constructed by averaging both the base and the candidate series at
220 each observation time if there was only one candidate series. For the situation with more than one
221 candidate series, the empirical orthogonal function (EOF) method was applied to these multiple
222 candidates and then the original fields were reconstructed with the leading principal components when
223 the accumulated variance explained by them exceeded 80%. This was expected to reduce the possible
224 impacts of abnormal observations and short-term discontinuities in the neighboring candidates on the
225 resultant reference series. Subsequently, the reference series were organized and constructed through
226 a spatial weighting scheme as each reconstructed record was assigned a spatially resolved weight
227 according to their relative distances to the base series over space. Here we applied a Gaussian kernel
228 function to estimate the weight of each neighboring observation that can influenced the base series in
229 space and such a scheme has been proven to be effective in assessing the spatial autocorrelation of
230 PM_{2.5} concentration (Bai et al., 2019b). Mathematically, the reference series can be constructed from
231 the following equations:

$$232 \quad PM_{ref} = \frac{\sum_{i=1}^N w_i * PM_{cand}^i}{\sum w_i} \quad (1)$$

$$233 \quad w = \exp\left(\frac{-d^2}{2h^2}\right) \quad (2)$$

234 where PM_{ref} and PM_{cand} denote the reference and candidate series, respectively. N is the total
235 number of candidate series while w is the spatially resolved weight assigned to each candidate series
236 and d is the spatial lag distance between the base and the corresponding candidate series. h is a spatial
237 correlation length that is used to modulate the relative influence of a distant observation on the data
238 measured at the base site. In this study, an empirical value of 50 km was used according to the estimated
239 semi-variogram results (Bai et al., 2019b).

240 For any record having neighboring series within 50 km but poorly correlated ($R < 0.8$ or $CV > 0.2$)
241 to all its neighbors (meaning the base series differ from the neighbors), the reference series were

242 created by following the same procedures as those detailed above by taking the nearest neighbor as the
243 base series. For the situation with only one candidate series available, it is logical to compare both the
244 base and the candidate series against another data to check which one should be corrected. In this study,
245 the $PM_{2.5}$ time series estimated from the MERRA-2 aerosol reanalysis in the same way as described
246 in He et al. (2019) was used. The one with higher correlation to this external $PM_{2.5}$ time series was
247 then used as the reference (deemed as homogeneous) while the other was considered as the base series
248 (i.e., implies to be adjusted). Such an inclusive scheme empowered us to screen and construct reference
249 series for 1,262 long-term $PM_{2.5}$ concentration records across the board. In contrast, no reference series
250 were constructed for 47 isolated records.

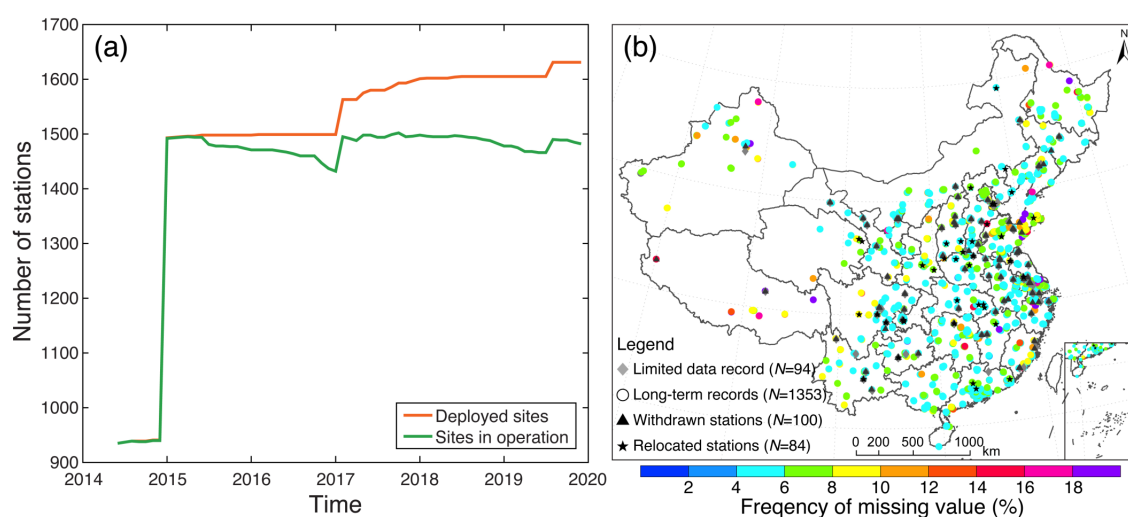
251 **3.3.2 Post-processing measures**

252 Several post-processing measures were applied to the adjusted data records to further improve
253 the quality of this dataset. Since nonpositive values may appear in the QM adjusted data series if the
254 original values are close to zero (Wang et al., 2010b), nonpositive values were replaced with the
255 smallest valid $PM_{2.5}$ concentration amount measured at each monitoring site during the study period.
256 Subsequently, the data gaps in the adjusted datum due to long-lasting missingness were filled by first
257 calibrating the corresponding data values in the reference series measured on the same date (if available)
258 to the homogenized datum level. The modified quantile-quantile adjustment (MQQA) method
259 proposed in Bai et al. (2016) was hereby used given its adaptive data adjustment principle. For the
260 predicted values, such MQQA scheme rendered higher accuracy than those interpolated from data
261 values measured on adjacent dates because $PM_{2.5}$ concentration is spatially more correlated than in the
262 temporal domain (Bai et al., 2019b). For the remaining data gaps, those missing values were
263 reconstructed in a similar procedure as the DCCEOF method (Bai et al., 2020b). Note that the matrix
264 used for EOF analysis in the context of DCCEOF was constructed using the neighboring data series
265 measured within a radius of 100 km with a temporal lag of 30 days at most. Finally, all data values
266 were rounded to integer to be in line with the original $PM_{2.5}$ concentration observations.

267 **4 Results and discussion**

268 **4.1 Descriptive statistics**

269 Prior to data homogenization, we first need to exclude those short-term and less reliable records.
 270 Figure 2 shows the temporal variations of the number of air quality monitoring stations deployed in
 271 China during 2015–2019 as well as the spatial patterns of the frequency of missing values for each
 272 long-term PM_{2.5} concentration record. It shows that a total of about 1,630 air quality monitoring
 273 stations had been deployed in China before 2020. Nevertheless, about 1,500 sites routinely providing
 274 PM_{2.5} observations were kept up in operation since 2015 (Figure 2a). By referring to the data continuity
 275 of PM_{2.5} observations, it is noticeable that 100 monitoring stations had been withdrawn before 2020
 276 because no PM_{2.5} observations were provided for more than three consecutive months since the release
 277 of their last valid data (Figure 2b). Meanwhile, 42 pairs of stations were found to be relocated since
 278 new stations at nearby started to provide PM_{2.5} observations soon after the suspension of the original
 279 site. This is also corroborated by the temporal lags of PM_{2.5} observations between original and newly
 280 deployed stations as many of them were found to have a time lag less than 15-day. Also, 94 sites were
 281 found with limited data records due to short temporal coverage (newly deployed). Finally, 1,353 long-
 282 term PM_{2.5} concentration records were identified with their first valid data released earlier than 2015.
 283 In regard to the frequency of missing value, it is indicative that data gaps were obvious in these long-
 284 term PM_{2.5} concentration records, with about 6% of hourly data values missed on ~47% of sampling
 285 days on average. This also motivates us to first fill such data gaps to improve the data integrity.



286
 287 **Figure 2.** Spatial and temporal patterns of air quality monitoring stations in China. (a) Temporal
 288 variations of the total number of air quality monitoring stations in China. (b) Spatial patterns of the
 289 frequency of missing value in each long-term hourly PM_{2.5} concentration record measured from

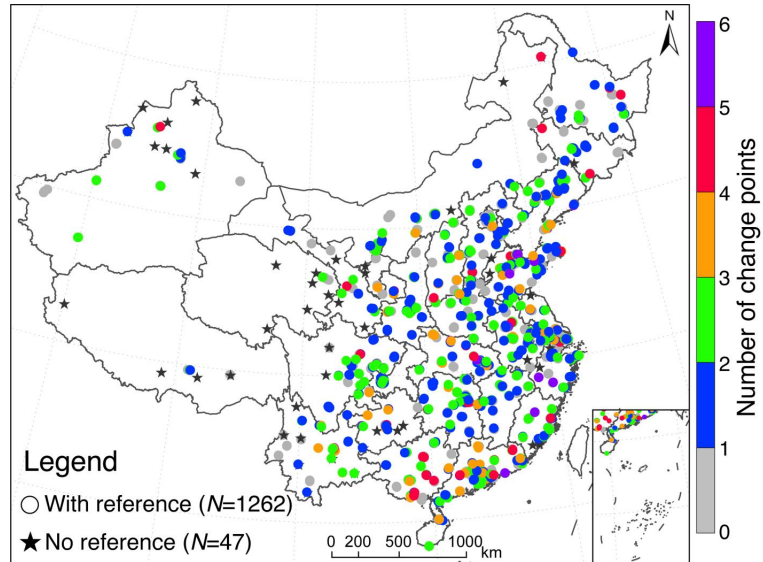
290 January 1, 2015 to December 31, 2019. Stations were categorized into distinct groups according to
291 their data length and temporal continuity. The frequency of missingness was calculated as the ratio of
292 the number of missing values in each PM_{2.5} concentration record to the total number of samplings from
293 the time of the release of the first valid data to December 31, 2019.

294 **4.2 Homogenization of *in situ* PM_{2.5} data**

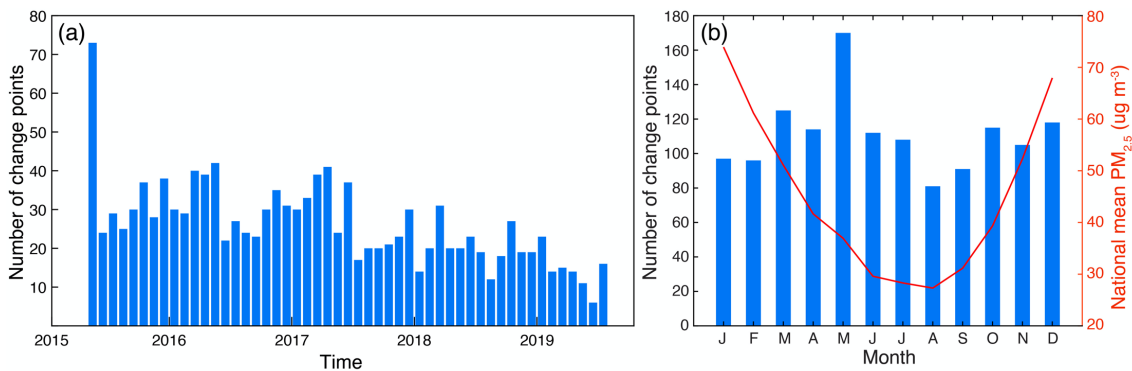
295 A total of 1,395 long-term (with five-year observations) PM_{2.5} concentration records were
296 acquired with the inclusion of 42 temporally merged data series at those relocated stations. After
297 removing those suffering from more than three consecutive months data losses, 1,309 long-term yet
298 consecutive PM_{2.5} concentration records were obtained. The homogeneity test was finally performed
299 on 1,262 records due to the availability of reference series. Figure 3 shows the spatial patterns of the
300 total number of change points detected in 1,262 monthly PM_{2.5} concentration records. The ubiquitous
301 change points imply that there is an obvious inhomogeneity in this *in situ* PM_{2.5} concentration dataset.
302 About 57% (719 out of 1,262) of records failed to pass the homogeneity test due to the presence of
303 change points. Given the overall good agreement between the base and reference series (refer to Figure
304 S1 for the correlation coefficient and root mean square error between them), it indicated that these PM_{2.5}
305 concentration records did suffer from evident discontinuities. Meanwhile, the vast majority (~80%) of
306 the inhomogeneous PM_{2.5} records suffered from no more than two change points (Figure 3), suggesting
307 the mean shift could be the primary reason for the detected discontinuities. Moreover, 20 records were
308 even found suffering from no less than five significant change points, indicating phenomenal
309 discontinuities in these records.

310 Figure 4 shows the temporal variability of the number of change points detected in monthly PM_{2.5}
311 concentration records. As indicated, change points were detected in every specific month of the year
312 from May 2015 to July 2019, especially in late spring (e.g., May), in which change points were more
313 likely to be detected (Figure 4b). This is attributable to the seasonality of PM_{2.5} loading in China as
314 high PM_{2.5} concentrations are always observed in the winter whereas low values in the summer.
315 Consequently, change points were more likely to be detected during the chronic transition periods (e.g.,
316 spring to summer). In addition, it is noteworthy that a large volume of change points was detected in
317 early 2015, indicating the existence of phenomenal discontinuities during this period (Figure 4a). After

318 checking the temporal variations of $PM_{2.5}$ concentration, findings indicate that $PM_{2.5}$ observations
 319 varied with large deviations among each other during this period. This could be linked to the imperfect
 320 instrument calibration or irregular operation in the early stage.



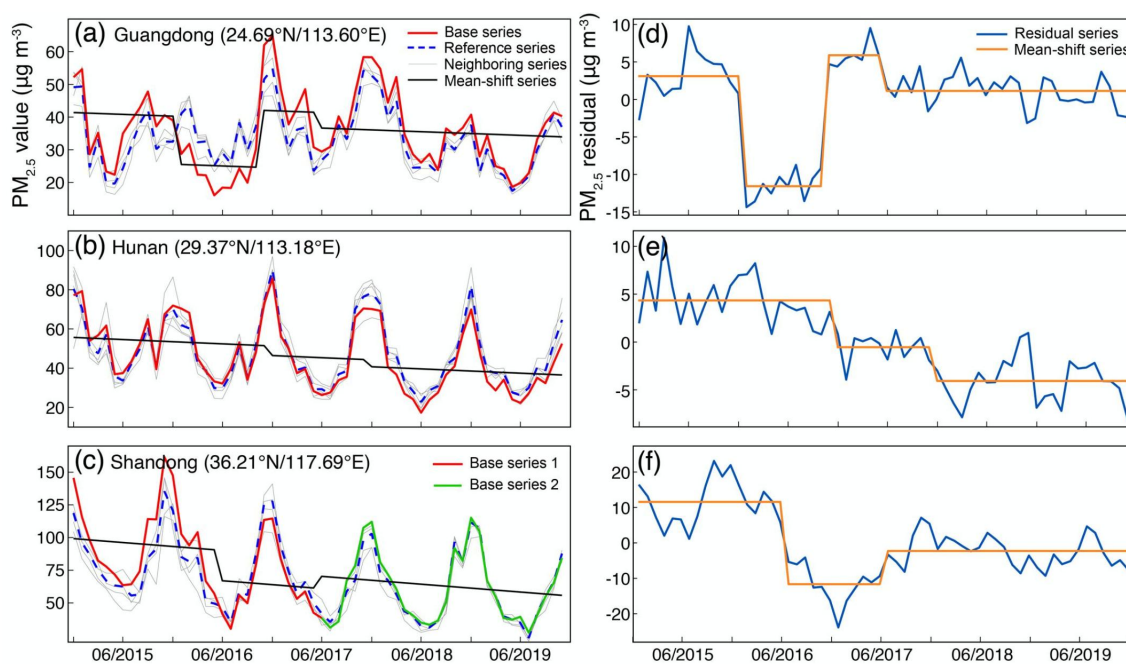
321
 322 **Figure 3.** Spatial patterns of the total number of change points detected in each long-term yet
 323 consecutive $PM_{2.5}$ concentration records. Gray dot indicates there was no change point detected in this
 324 $PM_{2.5}$ concentration record.



325
 326 **Figure 4.** Temporal variations of the number of change points detected in (a) each specific month from
 327 2015 to 2019 and (b) each month of the year. National mean $PM_{2.5}$ concentration in each month of the
 328 year was calculated based on $PM_{2.5}$ data measured at our selected 1309 sites during 2015–2019.

329
 330 Due to the lack of essential metadata information, it is a challenge for us to verify each detected
 331 change point through a manual inspection. Rather, the variations in the base and reference series was
 332 explored to identify the possible reasons for the detected discontinuities. Figure 5 presents three typical

333 inhomogeneous $PM_{2.5}$ time series with different number of change points. The inter-comparisons
 334 between the base and reference series indicate an overall good agreement among them in terms of the
 335 long-term variation tendency. However, obvious drifts were still phenomenal in their residual series,
 336 which were even more evident by referring to their mean-shift series. For example, both the residual
 337 and mean-shift series shown in Figure 5d clearly illustrate a typical discontinuity as there was an
 338 obvious departure of mean $PM_{2.5}$ concentration level during the period of January to October 2016. In
 339 contrast, the Figures. 5b and 5e present another typical inhomogeneity as statistically significant
 340 decreasing trend was found in the residual series with monthly $PM_{2.5}$ concentration deviations
 341 decreased from nearly $5 \mu g m^{-3}$ to $-4 \mu g m^{-3}$ step wise. Such inhomogeneity would undoubtedly result
 342 large bias in the trend estimations over that region. The bottom panel (Figures. 5c and 5f) shows the
 343 change points detected in the merged $PM_{2.5}$ time series at a pair of relocated sites. It is noteworthy that
 344 the detected discontinuity should be largely ascribed to the inconsistency emerged in the first data
 345 series rather than due to the site relocation.

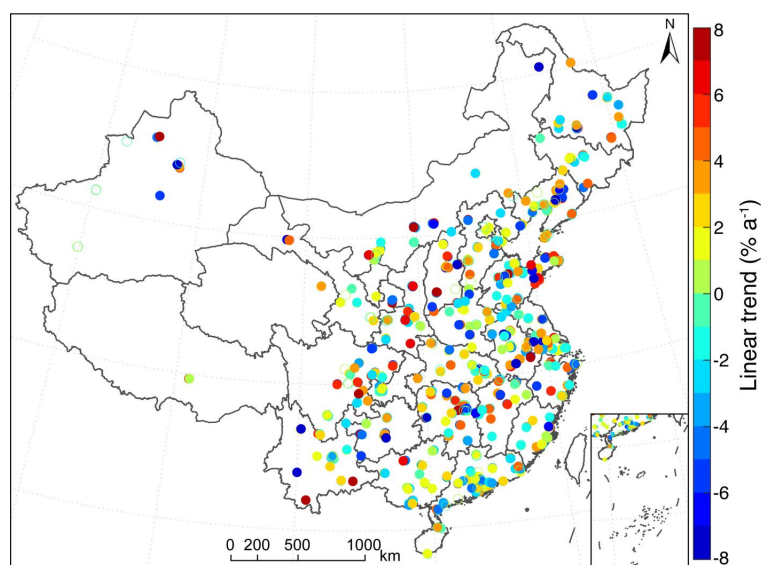


346
 347 **Figure 5.** Temporal variations of three typical inhomogeneous $PM_{2.5}$ concentration records during
 348 2015–2019. (Top) Significant deviations during a short time period, (middle) long-term chronic drifts
 349 with statistically significant varying trend detected in the residual series, (bottom) discontinuity due to
 350 site relocation. The left panel compares the base series with the reference and the neighboring series

351 used to compose the reference while the right panel shows the residual series between the base and
352 reference series as well as their mean-shift series.

353

354 Figure 6 shows the estimated linear trends for $PM_{2.5}$ residual series that failed to pass the
355 homogeneity test. Approximately 89% of the residual series were found exhibiting statistically
356 significant linear trends, suggesting the vital importance to homogenize such $PM_{2.5}$ concentration
357 records as the trend estimations at these stations could be prone to large bias if no essential adjustments
358 are performed. Further comparisons of the percentage of data gaps between homogeneous and
359 inhomogeneous records (Figure S2) as well as the spatial distance between the base and the reference
360 series (Figure S3) indicate that both the frequency of data gaps and spatial distance have no obvious
361 impact on the change point detection. In other words, the detected change points have no linkage with
362 neither missing value frequency nor spatial distance between the base and neighboring series,
363 suggesting a high confidence level of the identified discontinuities in these $PM_{2.5}$ concentration records.



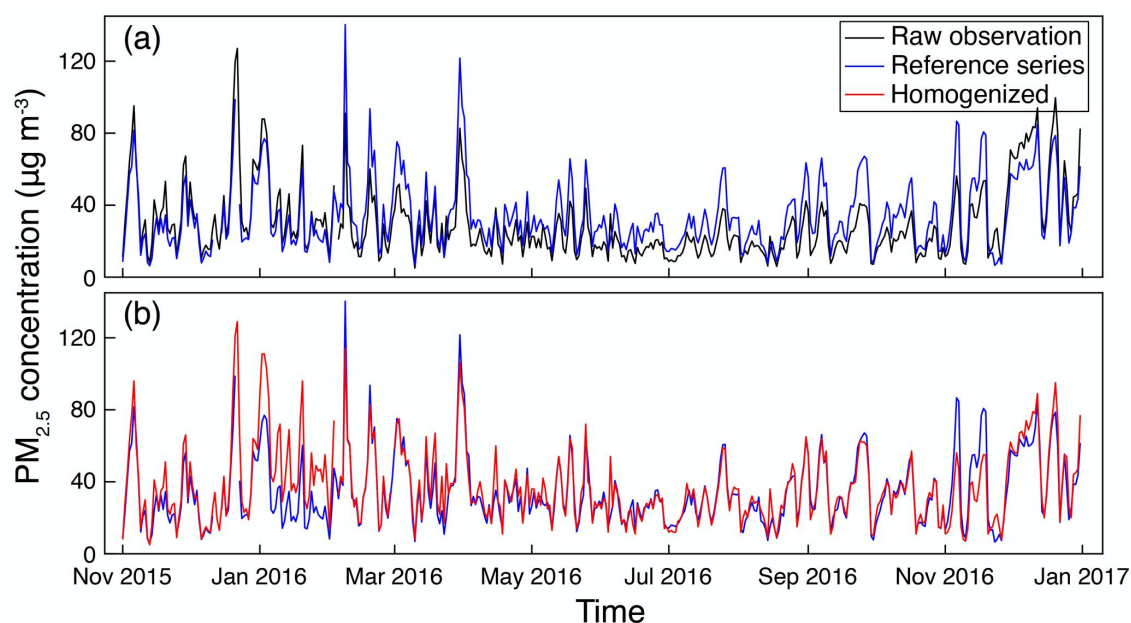
364

365 **Figure 6.** Trend estimations for the residual $PM_{2.5}$ concentration data series that failed to pass the
366 homogeneity test during 2015–2019. The solid circles indicate trends are statistically significant at the
367 95% confidence level.

368

369 Given the emergence of obvious discontinuities in more than half of the selected long-term $PM_{2.5}$
370 concentration records, the QM adjustment method was applied to correct the discontinuities detected

371 in each $PM_{2.5}$ concentration record. Figure 7 shows an example of homogenization on $PM_{2.5}$
 372 concentration data series that suffered from evident drifts from its reference (large drifts shown in
 373 Figure 5d). The inter-comparisons of $PM_{2.5}$ concentration data between the base and reference series
 374 indicate that the $PM_{2.5}$ concentration level was obviously underestimated by the raw observations
 375 compared with the reference, especially during the middle of 2016 (Figure 7a). Such evident drifts
 376 were remarkably diminished after the homogenization (Figure 7b), which shows a good agreement of
 377 the mean $PM_{2.5}$ concentration level between the homogenized datum and the reference series.

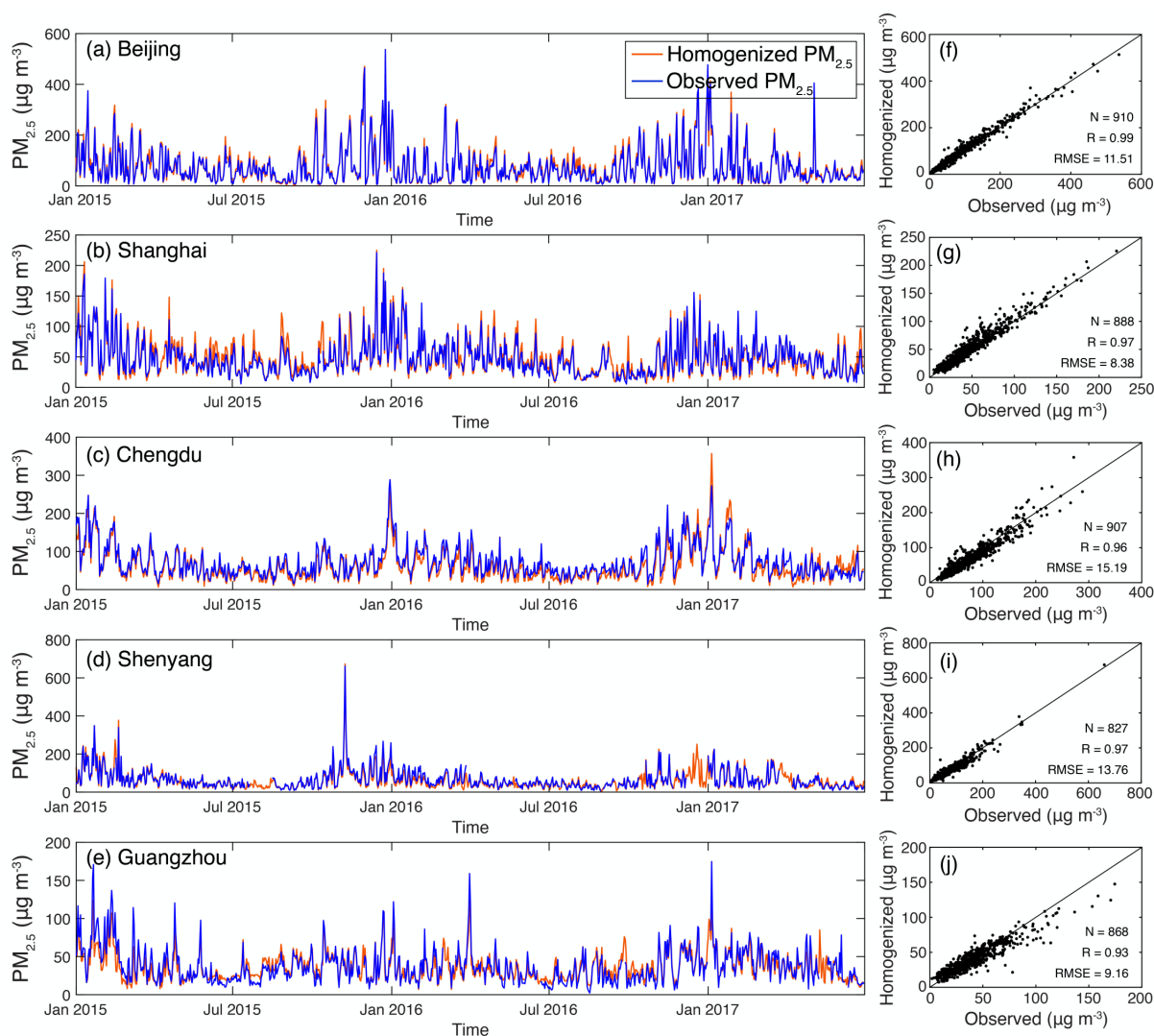


378
 379 **Figure 7.** Comparison of daily mean $PM_{2.5}$ concentration before and after homogenization at one
 380 monitoring site in Guangdong province ($24.69^{\circ}N/113.60^{\circ}E$) from November 2015 to December 2016
 381 (large drifts shown in Figure 5d).

382
 383 **4.3 Validation with independent dataset**

384 In this study, $PM_{2.5}$ observations that were collected independently by five consulates of United
 385 States distributed in five major Chinese cities between 2015 and 2017 were used to evaluate the
 386 consistency of the derived $PM_{2.5}$ concentration records. Figure 8 shows site-specific comparisons of
 387 daily $PM_{2.5}$ concentration between homogenized and observed data in Beijing, Shanghai, Chengdu,
 388 Shenyang, and Guangzhou, respectively. It is indicative that the homogenized daily $PM_{2.5}$
 389 concentration data were in good agreement with $PM_{2.5}$ observations sampled at US consulates, with a

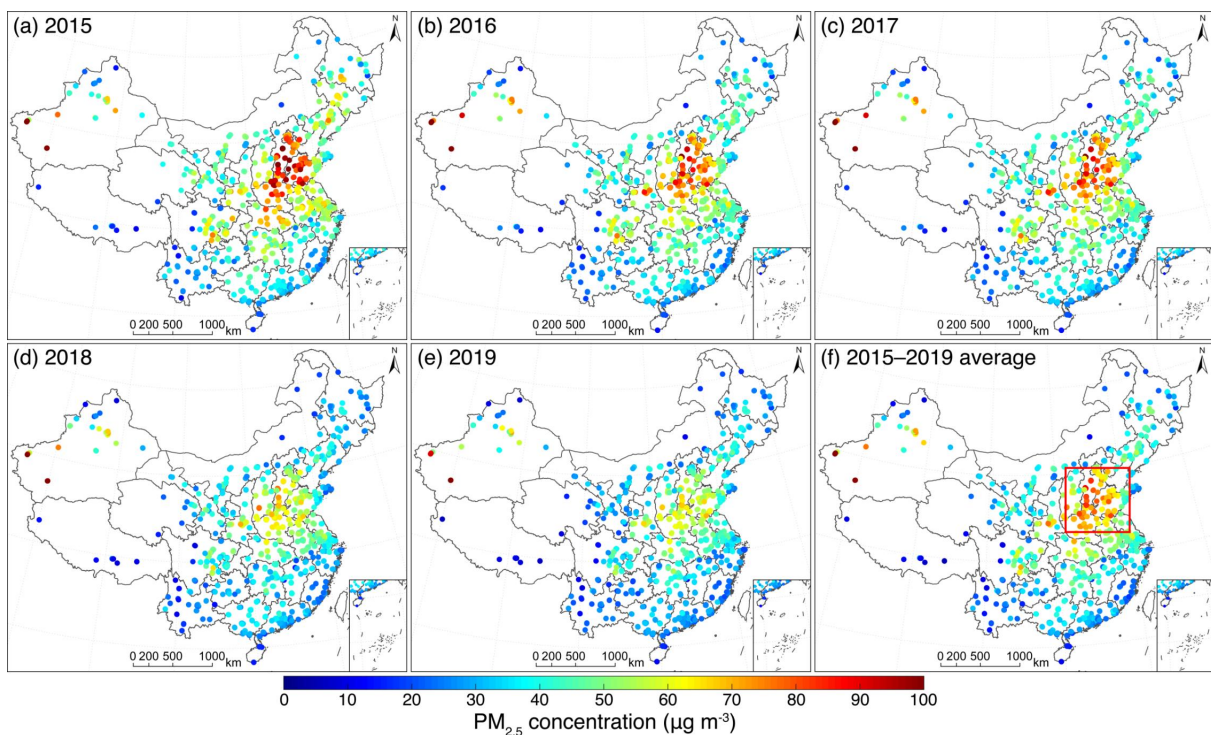
390 correlation coefficient value of >0.95 and root mean square error of $<15 \mu\text{g m}^{-3}$. Given the
 391 independent measurement of $\text{PM}_{2.5}$ concentration data at US consulates, we argue that the
 392 homogenized $\text{PM}_{2.5}$ records are accurate enough in characterizing the variability of $\text{PM}_{2.5}$ loadings in
 393 China. It is also noteworthy that the homogenized $\text{PM}_{2.5}$ records are temporally complete whereas
 394 missing values are found in $\text{PM}_{2.5}$ observations sampled at US consulates.



395
 396 **Figure 8.** Comparisons of the homogenized $\text{PM}_{2.5}$ concentration (red) against $\text{PM}_{2.5}$ observations (blue)
 397 measured at five consulates of United States in China from January 2015 to June 2017. (a–e) Temporal
 398 variations of daily $\text{PM}_{2.5}$ concentration and (f–j) the associated scatter plots.

399
 400 **4.4 $\text{PM}_{2.5}$ trends estimated from the homogenized dataset**

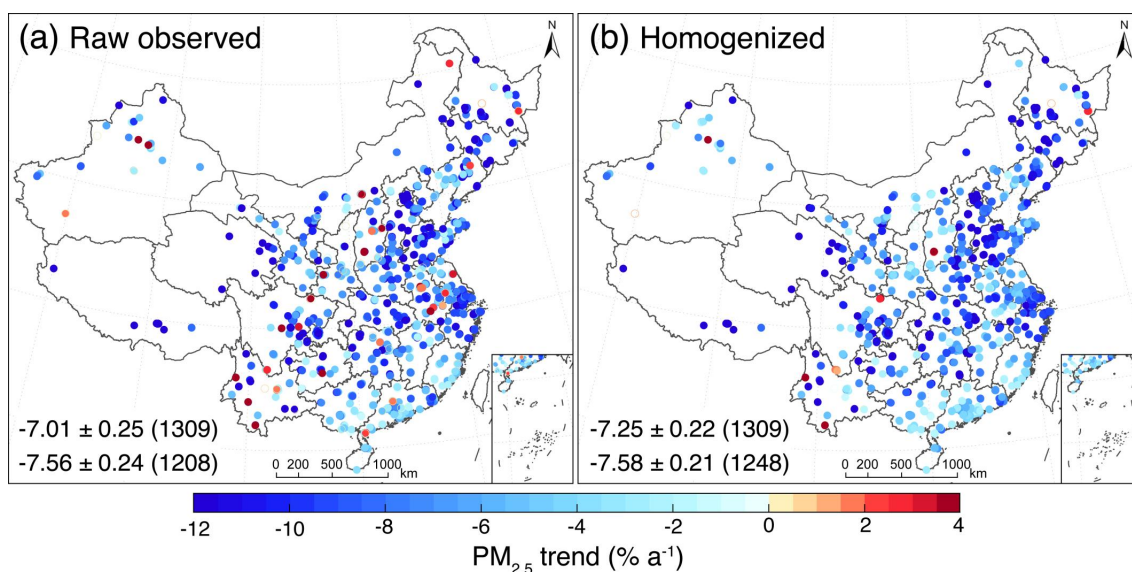
401 A homogenized data record is essential to trend analysis. Figure 9 presents the annual mean
 402 concentration of PM_{2.5} across China between 2015 and 2019. As shown, there is a phenomenal
 403 reduction of PM_{2.5} concentration in China in the past five years, especially over North China Plain (the
 404 region outlined by a red rectangle shown in Figure 9f) where the annual mean PM_{2.5} concentration
 405 decreased from more than 100 $\mu\text{g m}^{-3}$ in 2015 to about 60 $\mu\text{g m}^{-3}$ in 2019. Such an evident decrease in
 406 PM_{2.5} concentration clearly demonstrates the effectiveness of clean air actions that were implemented
 407 in recent years.



408
 409 **Figure 9.** Annual mean PM_{2.5} concentration derived from the homogenized daily PM_{2.5} concentration
 410 dataset at 1,309 monitoring stations in China between 2015 and 2019. The North China Plain was
 411 outlined by the red rectangle in panel (f).

412
 413 To evaluate the benefits of data homogenization on PM_{2.5} trend estimations, PM_{2.5} trends
 414 estimated from both the raw observations and homogenized dataset were compared. Prior to trend
 415 analysis, each PM_{2.5} concentration record was standardized in reference to its mean annual cycle (i.e.,
 416 PM_{2.5} concentration on the same date of the year between 2015 and 2019 was averaged) to reduce the
 417 impacts of seasonality and spatial variations. Figure 10 shows a site-specific comparison of PM_{2.5} trend
 418 estimations derived from raw observations and homogenized datasets during 2015–2019. In general,

419 trend estimations from both datasets showed an evident decreasing tendency of PM_{2.5} concentration
 420 across China during the study period. Nevertheless, noteworthy is that trend estimations derived from
 421 raw PM_{2.5} observations suffered from obvious inhomogeneity over space, being evidenced by
 422 antiphase (positive versus negative) trend estimations even at adjacent stations, especially for those
 423 with positive trends whereas all adjacent neighbors exhibited negative trends. These antiphase trend
 424 estimations over a small region also corroborate the existence of obvious inhomogeneity in raw
 425 observed *in situ* PM_{2.5} concentration dataset.



426

427 **Figure 10.** Linear trends for (a) raw observed and (b) homogenized daily PM_{2.5} concentration data
 428 during 2015–2019. Solid circles indicate trends are statistically significant at the 95% confidence
 429 interval. Numbers shown in the lower left of each panel indicate the overall trend derived from (top)
 430 all available stations and (bottom) the stations with significant trends at the 95% confidence interval
 431 while the numbers shown in brackets are the corresponding number of data records. Each PM_{2.5} time
 432 series were standardized by its mean annual cycle during the study period to account for spatial
 433 variations of PM_{2.5}.

434

435 The dotted antiphase trend estimations were substantially diminished after data homogenization,
 436 resulting in a spatially much more homogeneous decreasing tendency of PM_{2.5} concentration across
 437 China (Figure 10b). It is indicative that after data homogenization the national mean PM_{2.5} trend was
 438 enlarged from $-7.01\% \text{ a}^{-1}$ to $-7.25\% \text{ a}^{-1}$ while the uncertainty was reduced from $0.25\% \text{ a}^{-1}$ to $0.22\% \text{ a}^{-1}$

439 ¹. Also, the number of PM_{2.5} records with statistically significant trends was increased from 1,208 to
 440 1,248. These results collectively justify the effectiveness of the QM adjustment method in mitigating
 441 data inhomogeneity in PM_{2.5} observations, which also highlight the critical importance of data
 442 homogenization in accounting for discontinuities in this *in situ* PM_{2.5} concentration dataset. Overall,
 443 our results indicate an obvious decreasing trend of PM_{2.5} concentration in China in the past five years
 444 at a mean rate of $-7.25 \pm 0.22\% \text{ a}^{-1}$. Table 1 further compares the regional mean PM_{2.5} trend between
 445 2015 and 2019. Compared with other regions of interest (ROIs) such as Pearl River Delta (PRD, refer
 446 to Figure S4 for the location) and northern part of Xinjiang (XJ), PM_{2.5} loading over Beijing-Tianjin-
 447 Hebei (BTH), Heilongjiang-Jilin-Liaoning (HJL), and Central China (CC) decreased even more
 448 prominently.

449

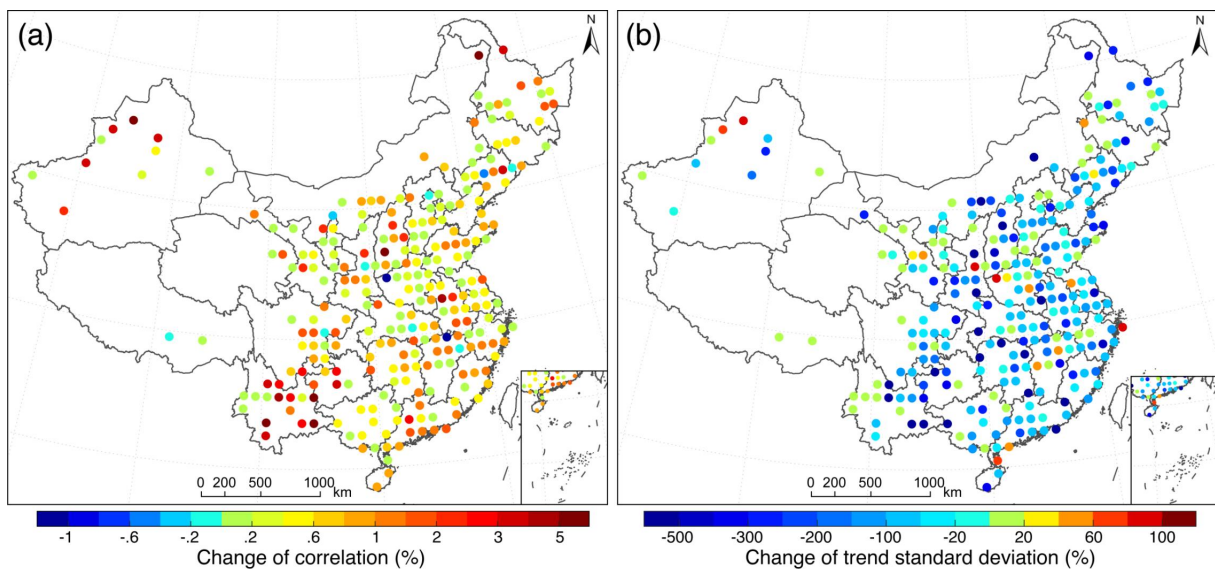
450 **Table 1.** Regional mean trend for PM_{2.5} concentrations over eight major ROIs in China during 2015–
 451 2019 before and after the data homogenization. Uncertainty in trend estimations were characterized at
 452 the 95% confidence interval. Locations of these ROIs can be found in Figure S4.

ROI	Raw observation (% a ⁻¹)	Homogenized record (% a ⁻¹)
Beijing-Tianjin-Hebei (BTH)	-9.03 ± 0.78	-9.19 ± 0.69
Yangtze River Delta (YRD)	-7.07 ± 0.54	-7.33 ± 0.40
Central China (CC)	-8.47 ± 0.51	-8.58 ± 0.41
Sichuan Basin (SCB)	-7.39 ± 1.02	-7.84 ± 0.89
Pearl River Delta (PRD)	-4.30 ± 0.51	-4.60 ± 0.39
Heilongjiang-Jilin-Liaoning (HJL)	-8.89 ± 0.73	-9.15 ± 0.63
Shaanxi-Gansu-Ningxia (SGN)	-4.85 ± 0.95	-5.30 ± 0.69
North Xinjiang (XJ)	-4.61 ± 1.96	-4.67 ± 1.60

453

454 To further assess the improvement of the data quality after homogenization, the daily *in situ*
 455 PM_{2.5} concentration records at a 1° × 1° grid cell resolution were grouped across China. In each grid
 456 cell, the regional mean correlation coefficient among PM_{2.5} concentration time series and standard
 457 deviation of PM_{2.5} trends were estimated from the raw observed and homogenized daily PM_{2.5}

458 concentration time series, respectively. Their relative differences were then calculated to show the
 459 improvements of data homogeneity within each grid cell. As shown in Figure 11, the correlation among
 460 PM_{2.5} concentration datum was enhanced ubiquitously after homogenization, especially in the
 461 southwest of China (e.g., Yunnan) where obvious inhomogeneity was observed in the raw PM_{2.5}
 462 observations (Figure 10a). Meanwhile, the standard deviation of PM_{2.5} trends within each grid cell was
 463 also substantially reduced, even by more than two folds in the magnitude (Figure 11b). These results
 464 also demonstrate the critical need to homogenize the observed PM_{2.5} concentration data from a large-
 465 scale monitoring network to reduce temporal inconsistency and spatial inhomogeneity that were not
 466 even noticed before.



467
 468 **Figure 11.** Spatial distributions of (a) the improvements of mean correlation coefficient among PM_{2.5}
 469 concentration records before and after homogenization at a 1° × 1° grid cell resolution across China,
 470 and (b) their corresponding standard deviations of PM_{2.5} trends.

471
 472 **5 Data availability**

473 The raw observations of *in situ* PM_{2.5} concentration data in China used in this study were
 474 retrieved via a web crawler from the National Urban Air Quality Real-time Publishing Platform
 475 (<http://106.37.208.233:20035>) between 2014 and 2019. Given the deployment of many new
 476 monitoring sites in 2014, we decided to generate a coherent PM_{2.5} concentration dataset starting from
 477 2015 to include as many PM_{2.5} data records as possible. The homogenized daily *in situ* PM_{2.5}

478 concentration dataset developed in this study is publicly accessible at
479 <https://doi.pangaea.de/10.1594/PANGAEA.917557> (Bai et al., 2020a). To provide a long-term
480 coherent PM_{2.5} concentration dataset to the scientific community, the homogenized PM_{2.5}
481 concentration dataset will be regularly updated for each half a year by including new PM_{2.5}
482 observations that are retrieved during the past six months.

483 **6 Conclusions**

484 In this study, a homogenized yet temporally complete daily *in situ* PM_{2.5} concentration dataset
485 was generated based on the discrete hourly PM_{2.5} concentration records that were retrieved from the
486 China National Urban Air Quality Real-time Publishing Platform using a web crawler during the
487 period of 2015–2019. To create such a long-term coherent dataset, a set of analytic methods were
488 geared up seamlessly and applied sequentially to the retrieved raw PM_{2.5} concentration records,
489 involving quality control, gap filling, data merging, change point detection, and bias correction. This
490 new dataset would help scientific community better elucidate the temporal and spatial variability of
491 haze pollution in China in the recent years, which is expected to improve the understanding of
492 underlying causes.

493 The raw PM_{2.5} concentration records were found to be suffering from phenomenal
494 inhomogeneity caused by data inconsistency and temporal discontinuity as well as the relocation and
495 repeal of a bunch of monitoring stations. More than half of the long-term PM_{2.5} concentration records
496 were found failing to pass the homogeneity test due to the presence of considerable change points.
497 Further investigation confirms that large yet short-term mean shifts and chronic drifts are two primary
498 reasons for the detected discontinuities in raw PM_{2.5} concentration records.

499 Based on the homogenized dataset, the long-term trends of PM_{2.5} concentration in China were
500 estimated. In contrast to the inhomogeneous trend estimations that were derived from raw PM_{2.5}
501 concentration records, the homogenized dataset yielded a spatially much more homogeneous
502 decreasing tendency of PM_{2.5} concentration across China at a mean rate of about –7.3% per year. Such
503 an improvement of homogeneity was also evidenced by the enhanced correlation and reduced standard
504 deviation of trend estimations between homogenized PM_{2.5} concentration time series in the

505 surroundings. These results clearly demonstrate the benefits of data homogenization on the
506 improvement of the quality of this PM_{2.5} concentration dataset as evident discontinuities have been
507 removed after homogenization. Overall, our results clearly indicate the presence of discontinuities in
508 the raw *in situ* PM_{2.5} concentration observations that were measured in China, and the homogenization
509 actions are essential to the acquisition of a long-term coherent PM_{2.5} concentration dataset that can be
510 used to advance PM_{2.5} pollution related policy making and public health risk assessment.

511

512 **Author contributions**

513 The study was completed with cooperation between all authors. JG and KB conceived of the idea
514 behind generating homogenous PM_{2.5} dataset across China; KB and KL conducted the data analyses
515 and KB wrote the manuscript; All authors discussed the experimental results and helped reviewing the
516 manuscript.

517 **Competing interests**

518 The authors declare that they have no conflict of interest.

519

520 **Acknowledgments**

521 This study was financially supported by the National Natural Science Foundation of China (grant
522 41701413), the National Key Research and Development Program of China (grant 2017YFC1501401),
523 and the International Cooperation Platform in Resources, Environment and Ecology, East China
524 Normal University. The authors are grateful to China National Environmental Monitoring Center
525 (<http://www.cnemc.cn/en/>) and the embassy of United States in China (<http://www.stateair.net/>) for
526 releasing the sampled air quality data publicly online. We also want to express our sincere thanks to
527 Dr. Yang Feng in the Expert Team on Climate Change Detection and Indices (ETCCDI)
528 (<http://etccdi.pacificclimate.org/software.shtml>) for providing the RHtestsV4 software package.

529

530 **References**

- 531 An, Z., Huang, R.J., Zhang, R., Tie, X., Li, G., Cao, J., Zhou, W., Shi, Z., Han, Y., Gu, Z., Ji, Y.,
532 2019. Severe haze in northern China: A synergy of anthropogenic emissions and atmospheric
533 processes. *Proc. Natl. Acad. Sci. U. S. A.* 116, 8657–8666.
534 <https://doi.org/10.1073/pnas.1900125116>
- 535 Anis, A.A., Lloyd, E.H., 1976. The Expected Value of the Adjusted Rescaled Hurst Range of
536 Independent Normal Summands. *Biometrika* 63, 111–116. <https://doi.org/10.2307/2335090>
- 537 Bai, K., Chang, N.-B., Yu, H., Gao, W., 2016. Statistical bias correction for creating coherent total
538 ozone record from OMI and OMPS observations. *Remote Sens. Environ.* 182, 150–168.
539 <https://doi.org/10.1016/j.rse.2016.05.007>
- 540 Bai, K., Chang, N.-B., Zhou, J., Gao, W., Guo, J., 2019a. Diagnosing atmospheric stability effects on
541 the modeling accuracy of PM_{2.5}/AOD relationship in eastern China using radiosonde data.
542 *Environ. Pollut.* 251, 380–389. <https://doi.org/10.1016/j.envpol.2019.04.104>
- 543 Bai, K., Li, K., Chang, N.-B., Gao, W., 2019b. Advancing the prediction accuracy of satellite-based
544 PM_{2.5} concentration mapping: A perspective of data mining through in situ PM_{2.5}
545 measurements. *Environ. Pollut.* 254, 113047. <https://doi.org/10.1016/j.envpol.2019.113047>
- 546 Bai, K., Li, K., Wu, C., Chang, N.-B., Guo, J., 2020a. A homogenized daily *in situ* PM_{2.5}
547 concentration dataset in China during 2015-2019. *PANGAEA*,
548 <https://doi.pangaea.de/10.1594/PANGAEA.917557>
- 549 Bai, K., Li, K., Guo, J., Yang, Y., Chang, N.-B., 2020b. Filling the gaps of in situ hourly PM_{2.5}
550 concentration data with the aid of empirical orthogonal function analysis constrained by diurnal
551 cycles. *Atmos. Meas. Tech.* 13, 1213–1226. <https://doi.org/10.5194/amt-13-1213-2020>
- 552 Bai, K., Ma, M., Chang, N.-B., Gao, W., 2019c. Spatiotemporal trend analysis for fine particulate
553 matter concentrations in China using high-resolution satellite-derived and ground-measured
554 PM_{2.5} data. *J. Environ. Manage.* 233, 530–542. <https://doi.org/10.1016/j.jenvman.2018.12.071>
- 555 Cai, W., Li, K., Liao, H., Wang, H., Wu, L., 2017. Weather conditions conducive to Beijing severe
556 haze more frequent under climate change. *Nat. Clim. Chang.* 7, 257–262.
557 <https://doi.org/10.1038/nclimate3249>

558 Cao, L.-J., Yan, Z.-W., 2012. Progress in research on homogenization of climate Data. *Adv. Clim.*
559 *Chang. Res.* 3, 59–67. <https://doi.org/10.3724/SP.J.1248.2012.00059>

560 Cao, L., Zhao, P., Yan, Z., Jones, P., Zhu, Y., Yu, Y., Tang, G., 2013. Instrumental temperature
561 series in eastern and central China back to the nineteenth century. *J. Geophys. Res. Atmos.* 118,
562 8197–8207. <https://doi.org/10.1002/jgrd.50615>

563 Ding, A.J., Huang, X., Nie, W., Sun, J.N., Kerminen, V.-M., Petäjä, T., Su, H., Cheng, Y.F., Yang,
564 X.-Q., Wang, M.H., Chi, X.G., Wang, J.P., Virkkula, A., Guo, W.D., Yuan, J., Wang, S.Y.,
565 Zhang, R.J., Wu, Y.F., Song, Y., Zhu, T., Zilitinkevich, S., Kulmala, M., Fu, C.B., 2016.
566 Enhanced haze pollution by black carbon in megacities in China. *Geophys. Res. Lett.* 43, 2873–
567 2879. <https://doi.org/10.1002/2016GL067745>

568 Guo, J.-P., Zhang, X.-Y., Che, H.-Z., Gong, S.-L., An, X., Cao, C.-X., Guang, J., Zhang, H., Wang,
569 Y.-Q., Zhang, X.-C., Xue, M., Li, X.-W., 2009. Correlation between PM concentrations and
570 aerosol optical depth in eastern China. *Atmos. Environ.* 43, 5876–5886.
571 <https://doi.org/10.1016/j.atmosenv.2009.08.026>

572 Guo, J., Xia, F., Zhang, Y., Liu, H., Li, J., Lou, M., He, J., Yan, Y., Wang, F., Min, M., Zhai, P.,
573 2017. Impact of diurnal variability and meteorological factors on the PM_{2.5}-AOD relationship:
574 Implications for PM_{2.5} remote sensing. *Environ. Pollut.* 221, 94–104.
575 <https://doi.org/10.1016/j.envpol.2016.11.043>

576 Guo, S., Hu, M., Zamora, M.L., Peng, J., Shang, D., Zheng, J., Du, Z., Wu, Z., Shao, M., Zeng, L.,
577 Molina, M.J., Zhang, R., 2014. Elucidating severe urban haze formation in China. *Proc. Natl.*
578 *Acad. Sci.* 111, 17373–17378. <https://doi.org/10.1073/pnas.1419604111>

579 He, L., Lin, A., Chen, X., Zhou, H., Zhou, Z., He, P., 2019. Assessment of MERRA-2 Surface PM_{2.5}
580 over the Yangtze River Basin: Ground-based verification, spatiotemporal distribution and
581 meteorological dependence. *Remote Sens.* 11. <https://doi.org/10.3390/rs11040460>

582 He, Q., Huang, B., 2018. Satellite-based mapping of daily high-resolution ground PM_{2.5} in China via
583 space-time regression modeling. *Remote Sens. Environ.* 206, 72–83.
584 <https://doi.org/10.1016/j.rse.2017.12.018>

585 Huang, X., Wang, Z., Ding, A., 2018. Impact of aerosol-PBL interaction on haze pollution: multiyear

586 observational evidences in North China. *Geophys. Res. Lett.* 45, 8596–8603.
587 <https://doi.org/10.1029/2018GL079239>

588 Li, Q., Zhang, H., Chen, J.I., Li, W., Liu, X., Jones, P., 2009. A mainland china homogenized
589 historical temperature dataset of 1951-2004. *Bull. Am. Meteorol. Soc.* 90, 1062–1065.
590 <https://doi.org/10.1175/2009BAMS2736.1>

591 Li, T., Shen, H., Yuan, Q., Zhang, X., Zhang, L., 2017. Estimating ground-level PM_{2.5} by fusing
592 satellite and station observations: A Geo-Intelligent deep learning approach. *Geophys. Res.*
593 *Lett.* 44, 11,985-11,993. <https://doi.org/10.1002/2017GL075710>

594 Li, Z., Guo, J., Ding, A., Liao, H., Liu, J., Sun, Y., Wang, T., Xue, H., Zhang, H., Zhu, B., 2017.
595 Aerosol and boundary-layer interactions and impact on air quality. *Natl. Sci. Rev.* 4, 810–833.
596 <https://doi.org/10.1093/nsr/nwx117>

597 Lin, C., Li, Y., Lau, A.K.H., Li, C., Fung, J.C.H., 2018. 15-Year PM_{2.5} trends in the Pearl River
598 Delta region and Hong Kong from satellite observation. *Aerosol Air Qual. Res.* 1–8.
599 <https://doi.org/10.4209/aaqr.2017.11.0437>

600 Lin, C.Q., Liu, G., Lau, A.K.H., Li, Y., Li, C.C., Fung, J.C.H., Lao, X.Q., 2018. High-resolution
601 satellite remote sensing of provincial PM_{2.5} trends in China from 2001 to 2015. *Atmos. Environ.*
602 180, 110–116. <https://doi.org/10.1016/j.atmosenv.2018.02.045>

603 Liu, D., Deng, Q., Zhou, Z., Lin, Y., Tao, J., 2018. Variation trends of fine particulate matter
604 concentration in Wuhan city from 2013 to 2017. *Int. J. Environ. Res. Public Health* 15, 1487.
605 <https://doi.org/10.3390/ijerph15071487>

606 Luan, T., Guo, X., Guo, L., Zhang, T., 2018. Quantifying the relationship between PM_{2.5}
607 concentration, visibility and planetary boundary layer height for long-lasting haze and fog–haze
608 mixed events in Beijing. *Atmos. Chem. Phys.* 18, 203–225. [https://doi.org/10.5194/acp-18-203-](https://doi.org/10.5194/acp-18-203-2018)
609 2018

610 Ma, Z., Hu, X., Sayer, A.M., Levy, R., Zhang, Q., Xue, Y., Tong, S., Bi, J., Huang, L., Liu, Y., 2015.
611 Satellite-based spatiotemporal trends in PM_{2.5} concentrations: China, 2004–2013. *Environ.*
612 *Health Perspect.* 124, 184–192. <https://doi.org/10.1289/ehp.1409481>

613 Nie, H., Qin, T., Yang, H., Chen, J., He, S., Lv, Z., Shen, Z., 2019. Trend analysis of temperature

614 and precipitation extremes during winter wheat growth period in the major winter wheat
615 planting area of China. *Atmosphere*. 10, 240. <https://doi.org/10.3390/atmos10050240>

616 Peterson, T.C., Easterling, D.R., 1994. Creation of homogeneous composite climatological reference
617 series. *Int. J. Climatol.* 14, 671–679. <https://doi.org/10.1002/joc.3370140606>

618 Rodriguez, D., Valari, M., Payan, S., Eymard, L., 2019. On the spatial representativeness of NO_x
619 and PM₁₀ monitoring-sites in Paris, France. *Atmos. Environ.* X 1, 100010.
620 <https://doi.org/10.1016/j.aeaoa.2019.100010>

621 Shen, H., Li, T., Yuan, Q., Zhang, L., 2018. Estimating regional ground-level PM_{2.5} directly from
622 satellite top-of-atmosphere reflectance using deep belief networks. *J. Geophys. Res. Atmos.*
623 2018JD028759. <https://doi.org/10.1029/2018JD028759>

624 Shi, X., Zhao, C., Jiang, J.H., Wang, C., Yang, X., Yung, Y.L., 2018. Spatial representativeness of
625 PM_{2.5} concentrations obtained using observations from network stations. *J. Geophys. Res.*
626 *Atmos.* 123, 3145–3158. <https://doi.org/10.1002/2017JD027913>

627 Wang, G., Zhang, R., Gomez, M.E., Yang, L., Levy Zamora, M., Hu, M., Lin, Y., Peng, J., Guo, S.,
628 Meng, J., Li, J., Cheng, C., Hu, T., Ren, Y., Wang, Yuesi, Gao, J., Cao, J., An, Z., Zhou, W., Li,
629 G., Wang, J., Tian, P., Marrero-Ortiz, W., Secrest, J., Du, Z., Zheng, J., Shang, D., Zeng, L.,
630 Shao, M., Wang, W., Huang, Y., Wang, Yuan, Zhu, Y., Li, Y., Hu, J., Pan, B., Cai, L., Cheng,
631 Y., Ji, Y., Zhang, F., Rosenfeld, D., Liss, P.S., Duce, R.A., Kolb, C.E., Molina, M.J., 2016.
632 Persistent sulfate formation from London Fog to Chinese haze. *Proc. Natl. Acad. Sci.* 113,
633 13630–13635. <https://doi.org/10.1073/pnas.1616540113>

634 Wang, X., Wang, K., 2016. Homogenized variability of radiosonde-derived atmospheric boundary
635 layer height over the global land surface from 1973 to 2014. *J. Clim.* 29, 6893–6908.
636 <https://doi.org/10.1175/JCLI-D-15-0766.1>

637 Wang, X.L., 2008a. Penalized maximal F test for detecting undocumented mean shift without trend
638 change. *J. Atmos. Ocean. Technol.* 25, 368–384. <https://doi.org/10.1175/2007JTECHA982.1>

639 Wang, X.L., 2008b. Accounting for autocorrelation in detecting mean shifts in climate data series
640 using the Penalized Maximal t or F Test. *J. Appl. Meteorol. Climatol.* 47, 2423–2444.
641 <https://doi.org/10.1175/2008JAMC1741.1>

- 642 Wang, X.L., Chen, H., Wu, Y., Feng, Y., Pu, Q., 2010a. New Techniques for the Detection and
643 Adjustment of Shifts in Daily Precipitation Data Series. *J. Appl. Meteorol. Climatol.* 49, 2416–
644 2436. <https://doi.org/10.1175/2010JAMC2376.1>
- 645 Wang, X.L., Chen, H., Wu, Y., Feng, Y., Pu, Q., 2010b. New techniques for the detection and
646 adjustment of shifts in daily precipitation data series. *J. Appl. Meteorol. Climatol.* 49, 2416–
647 2436. <https://doi.org/10.1175/2010JAMC2376.1>
- 648 Wang, X.L., Wen, Q.H., Wu, Y., 2007. Penalized maximal t test for detecting undocumented mean
649 change in climate data series. *J. Appl. Meteorol. Climatol.* 46, 916–931.
650 <https://doi.org/10.1175/JAM2504.1>
- 651 Wei, J., Li, Z., Cribb, M., Huang, W., Xue, W., Sun, L., Guo, J., Peng, Y., Li, J., Lyapustin, A., Liu,
652 L., Wu, H., Song, Y., 2020. Improved 1 km resolution PM_{2.5} estimates across China using
653 enhanced space – time extremely randomized trees. *Atmos. Chem. Phys.* 20, 3273–3289.
- 654 Xin, J., Wang, Y., Wang, L., Tang, G., Sun, Y., Pan, Y., & Ji, D., 2012. Reductions of PM_{2.5} in
655 Beijing-Tianjin-Hebei urban agglomerations during the 2008 Olympic Games. *Adv. Atmos.*
656 *Sci.*, 29(6), 1330–1342. <https://doi.org/10.1007/s00376-012-1227-4>
- 657 Xin, J., Wang, Y., Pan, Y., Ji, D., Liu, Z., Wen, T., Wang, Y., Li, X., Sun, Y., Sun, J., Wang, P.,
658 Wang, G., Wang, X., Cong, Z., Song, T., Hu, B., Wang, L., Tang, G., Gao, W., Guo, Y., Miao,
659 H., Tian, S., & Wang, L., 2015. The campaign on atmospheric aerosol research network of
660 China: CARE-China. *Bull. Am. Meteorol. Soc.* 96, 1137–1155. [https://doi.org/10.1175/BAMS-](https://doi.org/10.1175/BAMS-D-14-00039.1)
661 [D-14-00039.1](https://doi.org/10.1175/BAMS-D-14-00039.1)
- 662 Xu, W., Li, Q., Wang, X.L., Yang, S., Cao, L., Feng, Y., 2013. Homogenization of Chinese daily
663 surface air temperatures and analysis of trends in the extreme temperature indices. *J. Geophys.*
664 *Res. Atmos.* 118, 9708–9720. <https://doi.org/10.1002/jgrd.50791>
- 665 Yang, D., Wang, X., Xu, J., Xu, C., Lu, D., Ye, C., Wang, Z., Bai, L., 2018. Quantifying the
666 influence of natural and socioeconomic factors and their interactive impact on PM_{2.5} pollution
667 in China. *Environ. Pollut.* 241, 475–483. <https://doi.org/10.1016/j.envpol.2018.05.043>
- 668 Yang, Q., Yuan, Q., Yue, L., Li, T., Shen, H., Zhang, L., 2019. The relationships between PM_{2.5} and
669 aerosol optical depth (AOD) in mainland China: About and behind the spatio-temporal

670 variations. *Environ. Pollut.* 248, 526–535. <https://doi.org/10.1016/j.envpol.2019.02.071>

671 You, W., Zang, Z., Zhang, L., Li, Y., Wang, W., 2016. Estimating national-scale ground-level PM_{2.5}
672 concentration in China using geographically weighted regression based on MODIS and MISR
673 AOD. *Environ. Sci. Pollut. Res.* 23, 8327–8338. <https://doi.org/10.1007/s11356-015-6027-9>

674 Zhang, D., Bai, K., Zhou, Y., Shi, R., Ren, H., 2019. Estimating ground-level concentrations of
675 multiple air pollutants and their health impacts in the Huaihe River Basin in China. *Int. J.*
676 *Environ. Res. Public Health* 16, 579. <https://doi.org/10.3390/ijerph16040579>

677 Zhang, T., Zhu, Zhongmin, Gong, W., Zhu, Zerun, Sun, K., Wang, L., Huang, Y., Mao, F., Shen, H.,
678 Li, Z., Xu, K., 2018. Estimation of ultrahigh resolution PM_{2.5} concentrations in urban areas
679 using 160 m Gaofen-1 AOD retrievals. *Remote Sens. Environ.* 216, 91–104.
680 <https://doi.org/10.1016/j.rse.2018.06.030>

681 Zhao, P., Jones, P., Cao, L., Yan, Z., Zha, S., Zhu, Y., Yu, Y., Tang, G., 2014. Trend of surface air
682 temperature in Eastern China and associated large-scale climate variability over the last 100
683 years. *J. Clim.* 27, 4693–4703. <https://doi.org/10.1175/JCLI-D-13-00397.1>

684 Zheng, C., Zhao, C., Zhu, Y., Wang, Y., Shi, X., Wu, X., Chen, T., Wu, F., Qiu, Y., 2017. Analysis
685 of influential factors for the relationship between PM_{2.5} and AOD in Beijing. *Atmos. Chem.*
686 *Phys.* 17, 13473–13489. <https://doi.org/10.5194/acp-17-13473-2017>

687 Zou, B., Pu, Q., Bilal, M., Weng, Q., Zhai, L., Nichol, J.E., 2016. High-resolution satellite mapping
688 of fine particulates based on geographically weighted regression. *IEEE Geosci. Remote Sens.*
689 *Lett.* 13, 495–499. <https://doi.org/10.1109/LGRS.2016.2520480>

690